High Magnetic Field μSR Instrument

Scientific Case

October 21, 2005

A. Amato	**PSI**
S.J. Blundell	**U. Oxford**
S.F.J. Cox	**U. College, London**
E.M. Forgan	**U. Birmingham**
R.H. Heffner	**Los Alamos N.L.**
U. A. Jayasooriya	**U. East Anglia**
A. Keren	**Inst. of Technology, Technion-Israel**
H.-H Klauss	**T.U. Braunschweig**
T.N. Mamedov	**JOINT Institute, Dubna**
A. Schenck	**ETH Zurich**
V. Sechovsky	**Charles U., Prague**
G. Solt	**PSI**
A. Yaouanc	**CEA, Grenoble**

Preamble

Muons are very sensitive probes which have a large variety of applications in condensed matter and chemistry. With a magnetic moment larger than any nuclear moment, the muons are used to probe extremely small local magnetic fields, including their spatial distribution and temporal fluctuations, in any form of matter. In addition, the muon carries an electric charge and can be considered as a light proton, making it particularly useful for studying electronic quantum effects in matter. All these studies are performed with the μSR technique which utilizes the parity-violating decay of muons from a highly spin-polarized beam.

The number and diversity of phenomena studied by μSR has seen a remarkable growth over the last two decades. In Europe, the perfect complementarity between the *ISIS Pulsed Muon Facility* (Rutherford Appleton Laboratory, U.K.) and the continuous muon beam *PSI μSR Facility* ushered in a new era of exponential growth in techniques and applications of μSR.

At PSI, the μSR user community has established itself as one of the principal user communities. In 2005, about 80 research proposals of groups from PSI, Swiss universities and from abroad are active, using roughly 50% of the total beam time allocated to approved experiments at the target M and E beam lines. About 240 scientists from institutions in 22 countries are involved in the μSR proposals.

In the period 1995-2005, more than 550 articles, based on μSR work performed at PSI, have been published in internationally recognized journals, of which 47 articles appeared in prestigious journals as *Physical Review Letters, Science*, *Nature* and *J. American Chemical Society*. It is worth mentioning that this was achieved within the relatively modest budget of PSI μSR, reflecting a very high cost effectiveness of the Laboratory for Muon Spin Spectroscopy (LMU).

Since the year 2002, the PSI μSR Facilities take part in the framework programs of the European Commission *Transnational Access to Research Infrastructures*. Within this program, the LMU proposal has received ***top ranking*** by the EC experts who recognized the unique position of the PSI μSR Facility within the Condensed Matter and Chemistry communities.

To maintain its leadership in the field and to closely follow the internal and external user demands, the LMU is permanently enhancing the level of its μSR Facilities. Two aspects can be considered:

- improvements of the muon beam lines.
- improvements and developments of the μSR instruments.

For the first aspect, and in a recent past, two unique beam facilities have been realized or approved: i) the *Muon On REquest – MORE* facility and ii) a *high-intensity low-energy muon beam* to be installed in the former muE4 beam line.

Concerning the developments of the μSR instruments, much effort has been put recently on technical aspects as the improvement of the signal/background ratio, improved electronics, automatisation and user-friendliness. In parallel, and to cope with the increasing

demand of the users, the sample environment possibilities have been widely extended. A range of cryostats can be routinely used to cover temperatures between 0.02 to 900 K. External pressure up to 15'000 bars can now also be applied to the samples.

However, and partly due to the specificity of the μSR technique, the increasing demand on high magnetic fields (i.e. >> 1 Tesla), which has been observed among the main μSR users at PSI, could not be fulfilled due to the lack of a dedicated facility.
The purpose of this proposal is to present a *Scientific Case* in view of a realization of a high-field μSR Facility at PSI. It will provide the scientific motivation and future perspectives for the use of μSR with high magnetic fields.

The organization of this Scientific Case is as follows: In the Introduction, after some background information, the present and future situation of High-Field μSR will be shortly presented. Section 2 is devoted to the novel research becoming possible with a High-Field μSR instrument, with examples from the Condensed Matter, Chemistry and QED.

1 Introduction

1.1 Background

In order to gain more insight into the specific behavior of materials, it is often necessary to perform measurements as a function of different external parameters. Despite its high sensitivity to internal fields, this simple observation also applies for the μSR technique.

The most common parameter which can be tuned during an experiment is the sample temperature. By using a range of cryostats, temperatures between 0.02 and 900K can be covered at the PSI μSR Facility. On the other hand, and by using high-energy muons, pressures as high as 10'000 bars can nowadays be reached during μSR experiments [1].

As will be demonstrated in the following Sections, the magnetic field is an additional external parameter playing a fundamental role when studying the ground state properties of materials in condensed matter physics and chemistry. However, the availability of high magnetic fields for μSR experiments is still rather limited. Hence, if on one hand the high value of the gyromagnetic ratio of the muon ($\gamma_\mu = 2\pi \cdot 135.54 \cdot 10^6$ Rad s^{-1} $Tesla^{-1}$) provides the high magnetic sensitivity of the method, on the other hand it can lead to very high muon-spin precession frequencies when performing measurements in applied fields (the muon-spin precession frequency in a field of 1 Tesla is 135.5 MHz). Consequently, the use of ultra-fast detectors and electronics is mandatory when measuring in magnetic fields exceeding 1 Tesla. If such fields are very intense when compared to the Earth magnetic field ($< 1 \cdot 10^{-4}$ Tesla), the energy associated with them is still modest in view of the thermal energy. Hence, the Zeeman energy splitting of a free electron in a magnetic field of 1 Tesla corresponds to a thermal energy as low as 0.67 Kelvin. It is worth mentioning that nowadays magnetic fields of the order of 10 to 15 Tesla are quite common in condensed matter laboratories and have opened up vast new exciting experimental possibilities.

1.2 Present Situation of High-Field μSR

Among the μSR user community a rising demand to perform μSR studies under high magnetic fields is clearly noticeable. This predominantly applies for the two existing research centers world-wide where continuous muon flux are available and *high-field transverse-field* μSR experiments are feasible, TRIUMF (Canada) and PSI.

To cope with this increasing demand, a new μSR instrument ("BELLE") has recently been installed at the TRIUMF μSR Facility [2]. Serving primarily the North-American (and partially the Japanese) μSR community, this instrument, which can be operated at 7 Tesla, has established the technical practicability of μSR measurements under high magnetic fields.

At PSI, the highest magnetic field for μSR experiments in transverse field configuration is available at the *Low Temperature Facility* (LTF). This facility is equipped, in addition to a ^{3}He-^{4}He dilution refrigerator, with a split-coil Helmoltz superconducting magnet reaching up to 3 Tesla. On the remaining PSI μSR instruments transverse magnetic fields of the order of 0.5 Tesla are routinely accessible.

Though the LTF facility should predominantly be dedicated to extremely low temperatures (i.e. < 1K), its specific magnet configuration has led to a growing and recurrent

"misuse" of this facility, with solely its field capability being exploited. Moreover, the muon and positron detectors installed in the LTF cryostat are characterized by a relatively limited time resolution (ca. 1 ns) which leads to a gradual loss of the μSR signal with increasing field and significantly hampers studies at magnetic field above 2 Tesla (see Figure 1).

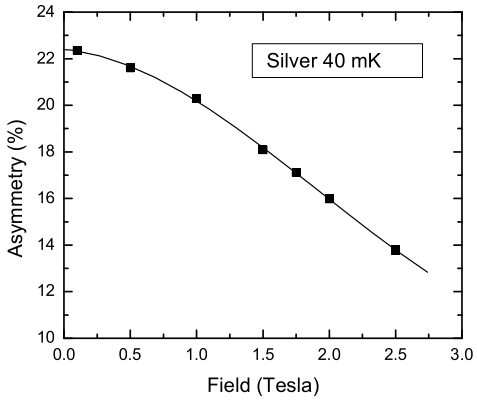

Figure 1 *Decrease of the μSR signal amplitude with increasing magnetic field measured in the LTF instrument at PSI.*

The remaining μSR centres (KEK, Japan and ISIS, U.K) are characterized by pulsed muon beams providing very limited time resolution. In such facilities, μSR transverse-field studies are only possible with fields as low as about 0.2 Tesla. On the other hand, and owing to the very low background, such facilities are suitable to study the spin–lattice relaxation phenomena, which are monitored by the muon-spin relaxation and consist of an energy exchange between the spins of the investigated systems and the two muon Zeeman levels. In such pulsed muon μSR facilities, high *longitudinal-field* studies can therefore be employed to gain more insight into the temporal fluctuations of the spins inside the investigated systems (see also Section 2.4.2). However, no high-field facilities are currently available at pulsed muon beams.

1.3 Future of High-Field μSR Outside of PSI

As shown in the following, it emerges clearly that the magnetic field will be considered in the next future as a standard parameter to choose during μSR studies. In addition to the foreseen high-field μSR Facility at PSI, several projects world-wide are presently considered to cope with the user demand.

As already mentioned, the TRIUMF high-field instrument has clearly opened up a vast area of new μSR research and has demonstrated the feasibility of the technique. Nevertheless, this instrument suffered from the fact that it was built around a recycled superconducting magnet which is missing the necessary high stability for specific μSR studies. To cope with this situation, a replacement of the magnet has been recently decided.

On the side of pulsed muon beam facilities, a high longitudinal-field instrument is projected at the ISIS Pulsed Muon Facility. At the present stage of the project, two field configurations are investigated, i.e. 3 and 7 Tesla. It is planned that specific funding for this new instrument will be requested from the Engineering and Physical Sciences Research Council (EPSRC, U.K.).

It must be stressed that the foreseen PSI high-field facility is perfectly complementary to the U.K. project. As demonstrated in the following Sections, the foreseen research at PSI will be focused on studies making primarily use of the transverse-field μSR technique, which are *not feasible* at the ISIS facility. In addition, the PSI high-field facility is foreseen to be equipped by a more intense magnet reaching almost 15 Tesla. In this vein, the PSI project will not only preserve the scientific leadership of the PSI users community in the field of μSR, but will also provide an important European added value by establishing, together with the U.K. project, a real and complementary European μSR Facilities network. This aspect is clearly recognized by both European μSR facilities which, together with different universities, have commonly seeked specific R&D funds dedicated to high-field μSR within the 6th framework program of the European Commission (*Research and Technical Developments* Networks, within the *Neutrons and Muons* Integrate Infrastructure Initiative – "NMI3") which started in 2004.

2 New Research Possible with a High-Field μSR Instrument

The present Section will focus on some examples of foreseen research which could be performed at a future high-field μSR facility at PSI. These examples constitute a short and incomplete summary of the Workshop *Towards a High Magnetic Field μSR Facility* which was held at PSI on January 15-16, 2002 and which was attended by about 50 representatives of different European research groups.

2.1 Condensed Matter

2.1.1 Superconductors

2.1.1.a Flux Line Lattice - Synergy μSR / SANS

When a high enough magnetic field is applied to a *type-II* superconductor (one in which the magnetic field penetration depth is larger than the size of the Cooper pairs of electrons), the field enters in the form of quantized flux lines, each carrying $h/2e$ of magnetic flux. In the simplest case, these lines will pack together to form a lattice of triangular symmetry. However in many cases this does not occur: the *shape* (triangular, square or distorted) of the flux line lattice (FLL) contains information about the *shape* of the flux lines themselves. This may reflect the interaction between the FLL and the crystal lattice, or even more interestingly, may contain information about the nature of the pairing mechanism in the superconducting state.

For instance, there is a tendency for a square FLL to occur at high fields in a *d-wave* superconductor [3]. An unconventional superconductor of this type has the electrons in a Cooper pair with antiparallel spins (as in a conventional *s-wave* superconductor), but with 2 units of relative angular momentum. The energy required to break a Cooper pair in such a superconductor varies around the Fermi surface, with fourfold symmetry. The nature of the pairing in unconventional superconductors is revealed not only by the FLL symmetry, but even more strongly and characteristically in the detailed variation of the magnetic field *B(r)* around the cores of the flux lines.

The microscopic properties of FLLs may be observed both by small-angle neutron scattering (SANS) and by μSR. SANS gives a very *visual* indication - as a diffraction pattern - of the symmetry of the FLL, but cannot without further information provide *B(r)*. The μSR technique directly gives the distribution of *values* of magnetic field in the FLL and in many cases this reflects the FLL symmetry and the value of the magnetic penetration depth. However, if insight from *both* measurements is combined, much more information can be obtained from either alone, and the explicit spatial variation *B(r)* may be obtained.

A (low field) demonstration of the possibilities in the (probably *p*-wave) superconductor Sr_2RuO_4 is given in Ref. 4. In this material, the FLL is square and in addition the *shape* of the flux lines, as revealed by the measurements, is highly unconventional. This is believed to be a reflection of the underlying pairing, which is probably not just *p*-wave (parallel spins, with one unit of relative angular momentum), but also breaks time-reversal symmetry!

Many other unconventional superconductors have *large* values of the upper critical field, above which superconductivity is destroyed. Among these are organic, heavy fermion and high-T_c superconductors. There are many other high-field superconductors of great interest, even if their pairing is fairly conventional, such as the rare earth borocarbides and MgB_2. There is therefore a need to combine the insights obtained from high field SANS with those from μSR at similar fields. At PSI there is now based a SANS magnet capable of 11 Tesla, which is far above the usual 0.6 Tesla in e.g. the GPS μSR instrument. A very productive area of research would be opened up by the ***synergy*** between high field μSR and SANS in the investigation of flux lines in superconductors.

2.1.1.b Field Dependence of the Length Scales

As said, an external magnetic field B_{ext} such that $B_{c1} < B_{ext} < B_{c2}$ (where B_{c1} and B_{c2} represent the characteristic critical fields of the superconducting material) will penetrate in a superconductor of *type II* in the form of flux tubes. Two length scales characterize a *type II* superconductor: i) the radius of the flux tubes which can be associated to the Ginzburg coherence length (ξ) and ii) the London penetration length (λ) which gives the distance over which the screening currents around a flux tube vanish. From conventional theories, it is expected that these two length scales are field independent.

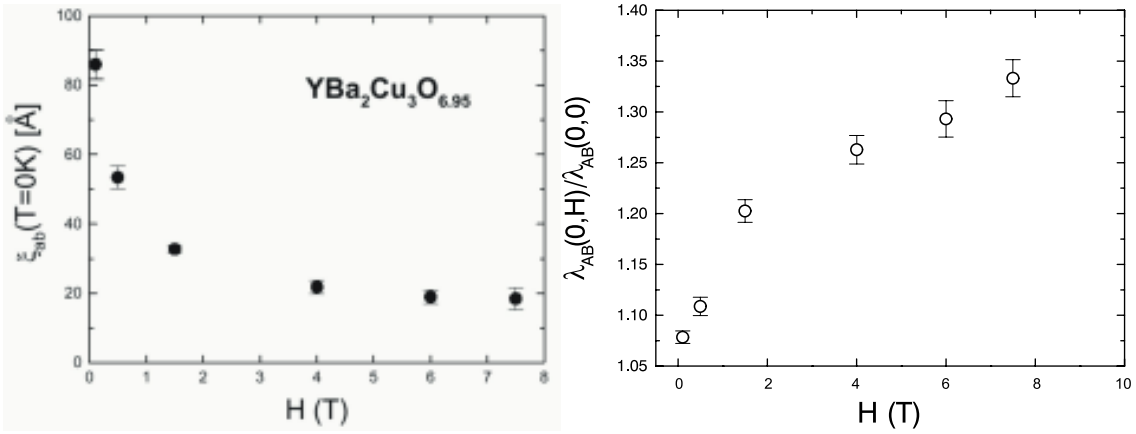

Figure 2 *Field dependence of the Ginzburg-Landau coherence length and London length extrapolated to T = 0K for $Yba_2Cu_3O_{6.95}$; from J.E. Sonier et al. [6].*

μSR is a unique technique to *simultaneously* obtain information on both length scales, and numerous studies were devoted to this topic [see Ref. 5 for a review]. Generally speaking, λ can be ascertained by a measurement of the transverse field linewidth in the superconducting state. The coherence length ξ is determined by a careful measurement of the lineshape in transverse field, together with a fit to a model of the internal field distribution from the superfluid flux lattice. Experiments in the high temperature superconductor $Yba_2Cu_3O_{6.95}$ up to $B_{ext} \cong 8$ T have found that ξ (or somewhat equivalently, the radius of the fluxoid cores) shrinks in applied fields [5]. This effect can be thought of as a reduction of lost condensation energy due to an increasing normal state volume as the number of vortices increases with increasing applied field. Measurements of λ as a function of field $B \leq 10$ T in $Yba_2Cu_3O_{6.95}$ show that λ increases in field due to non-local effects, which alter the field near

the vortex cores [6] (see Figure 2). Similar data were obtained for the system $NbSe_2$ [7]. In order to test the role of the crystallographic anisotropy on these observations, μSR measurements were performed on the cubic compound V_3Si. They revealed that the London length is independent of the field strength, but the Ginzburg coherence length was still found to be field dependent [8]. These apparently contradictory results have triggered different studies with the aim to obtain a complete picture of the field dependence of these two length scales. However, such studies will obtain quantitative results only when fields of the order of, at least, a fraction of B_{c2} will be used. In view of the large values of B_{c2} observed in novel superconductors (e.g. heavy-fermions, organics, high-T_c) such μSR studies will require the use of fields of the order of 10 Tesla.

2.1.1.c Organics Superconductors

Layered organic superconductors based on the molecule bis(ethylenedithio)-tetrathiafulvalene, also known as BEDT-TTF, are currently of enormous interest [9] because of their low dimensionality, chemical tuneability, and because there is growing evidence that their superconductivity is *unconventional*.

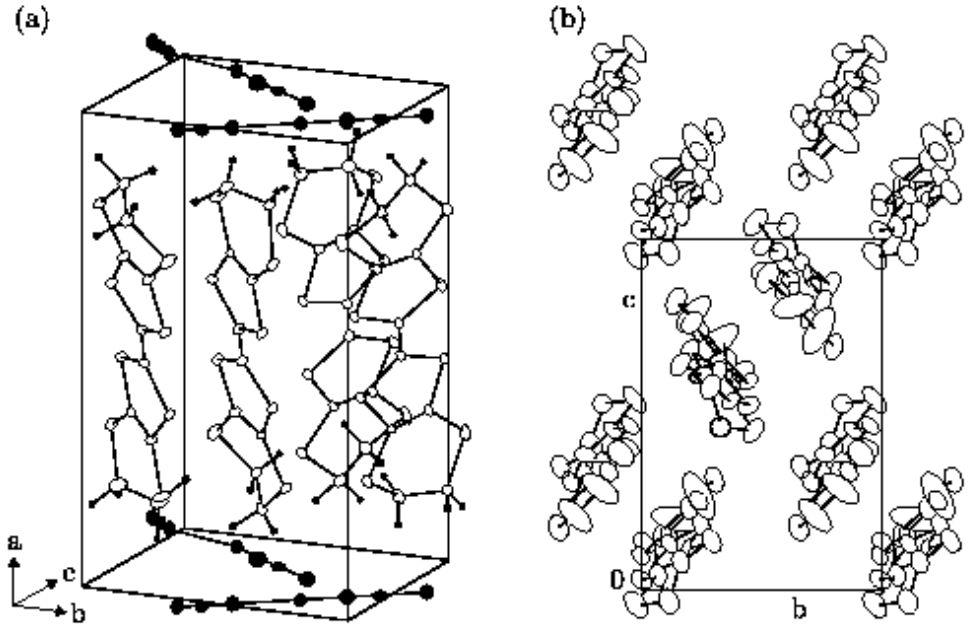

Figure 3 *An organic superconductor consists of alternating layers of organic molecules and inorganic anions. The figure shows* ***(a)*** *a side-view and* ***(b)*** *a plan-view of* κ-$ET_2Cu(SCN)_2$.

In these materials, BEDT-TTF molecules are stacked next to each other to ensure that the molecular orbitals overlap. Generally, a number *n* of BEDT-TTF molecules jointly donate an electron to a second type of molecule (*X*) to form a compound $(BEDT\text{-}TTF)_nX$; *X* is known as the anion, while the BEDT-TTF molecule is referred to either as the donor or cation. The transfer of charge serves to bind the charge-transfer salt together (in a manner analogous to ionic bonding) and also leaves behind a hole, jointly shared between the *n* BEDT-TTF molecules [9]. This means that the bands formed by the overlap of the BEDT-

TTF molecular orbitals will be partially filled, leading one to expect that the charge-transfer salt will conduct electricity.

The low dimensionality of the resulting salts leads to a large (but tuneable) degree of anisotropy in the superconducting properties and produces an *extremely rich temperature–magnetic field phase diagram*. In the following we enumerate some specific research topics where a future high-field μSR instrument could play a key role.

In highly anisotropic systems the vortex lattice is not a system of rigid rods (as in the isotropic case) but should be considered as a weakly coupled stack of quasi-two-dimensional (q2D) "pancake" vortices, each one confined to a superconducting plane. The phase diagram is thus substantially altered to take account of field and temperature dependent changes in the vortex lattice itself. At low temperature (T) and low magnetic field (B) the stacks resemble conventional vortex lines. Above a characteristic temperature T_b, but still below that at which superconductivity is destroyed, the vortex lattice is broken up by thermal fluctuations (vortex lattice melting). At low T, but this time increasing B, the energetic cost of interlayer deformations of the lattice (local tilting of the lines) is progressively outweighed by the cost of intralayer deformations within the superconducting plane (shearing). Above a crossover field B_{cr} the vortex lattice enters a more two-dimensional regime. Thus in anisotropic systems we may expect *temperature and field dependent transitions* in which the vortex lattice is destroyed and these can be effectively probed using μSR. As an example, such studies in κ-$ET_2Cu(SCN)_2$ demonstrate the existence of a flux-line lattice only at low fields [10], with a transition to q2D order with reduced correlations of vortex segments along the field direction. In addition, the μSR results demonstrate that the order parameter of κ-$ET_2Cu(SCN)_2$ contains line nodes, thus ruling out a conventional *s*-wave interpretation for this material [11].

The high purity and quality of ET based organic superconductors permits the measurement of Fermi surface parameters using the de Haas–van Alphen and Shubnikov–de Haas effects, and this has led to many advances in experimental 'fermiology' of organic metals [9]. Angle-dependent magnetoresistance measurements have demonstrated the coherence of the Fermi surface in the interlayer direction [12]. A high-field muon spectrometer could allow one to measure diamagnetic domains [see 13 and Section 2.1.2.d] for the first time in an organic superconductor.

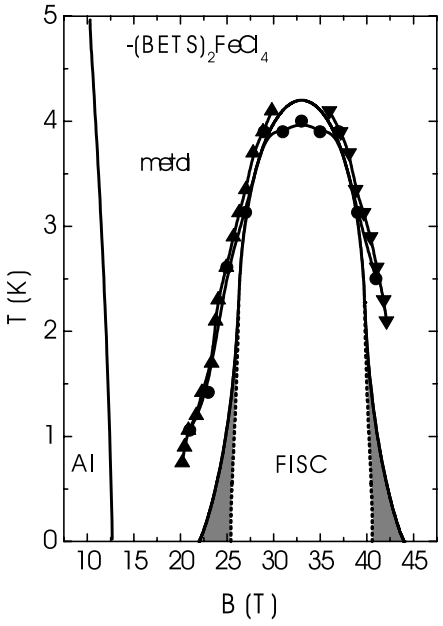

Figure 4 *λ-phase of $BETS_2FeCl_4$: the Jaccarino-Peter effect is at play [15].*

The transition temperature of many ET superconductors falls with applied pressure, so negative pressure can be applied chemically by making the ET molecular larger. Partial substitution of sulphur atoms by selenium produces the molecule BEDT-TSF (abbreviated to BETS) and some superconductors using this molecule have been found. BETS superconductors provide an opportunity to study the interplay of magnetism and superconductivity; several salts of the form $BETS_2X$ are superconductors where X is a magnetic anion. In particular, this is the case for the κ phase with $X = FeBr_4$ and $FeCl_4$. In the salt with $FeBr_4$, the Fe^{3+} is in a high-spin state

(S = 5/2) and the salt undergoes an antiferromagnetic transition at T_N = 2.5K and a superconducting transition at T_c = 1K. For the $FeCl_4$ salt the two transitions are reduced in temperature by a factor of 5–10. It is predicted that the interaction between localized and delocalized states in the κ phase salts leads to a commensurate spin-density wave state in the molecular layers in addition to the ordering of the Fe. Since the μSR technique provides microscopic information on both the magnetic and the superconducting states, measurements in high field could be used to gain insight into the specific interplay between both phenomena.

Another example of possible application of high-field studies in organic superconductors is furnished by the λ-phase of $BETS_2FeCl_4$. In zero magnetic field, λ-$BETS_2FeCl_4$ shows a metal-insulator transition around 8K associated with antiferromagnetic order. This insulating phase is destabilized in magnetic fields above 10 Tesla. When a large magnetic field is applied exactly parallel to the conduction planes in λ-$BETS_2FeCl_4$, superconductivity is induced above 17 Tesla below 1K (see Figure 4) [14,15] which is believed to be associated with a Jaccarino-Peter effect [16] in which the applied field cancels the exchange interaction with localized Fe moments. Though the field to induce superconductivity is large, it can be reduced by forming alloys such as $BETS_2Fe_xGa_{1-x}Cl_yBr_{1-y}$ [17].

2.1.1.d New Physics

The examples discussed so far concern studies that could have been undertaken at PSI in the recent past if magnetic fields in the range of $B \leq 15$ T had been available. We now discuss a case in which new physics could be investigated in the future in the field of superconductivity.

Suppose we wish to study phenomena near the upper critical field B_{c2}. Using the BCS estimate [18] for $B_{c20} = \phi_0 / 2\pi\xi^2$, where $\xi = \hbar v_F/\pi\Delta$ is the coherence length, $\Delta = 1.76 k_B T_c$ is the energy gap parameter, and $\phi_0 = 2\ 10^{-7}$G·cm^2, one can show that $B_{c20} \propto T_c^2/\varepsilon_F$, where ε_F is the Fermi energy (corresponding to the Fermi velocity v_F). Ordinary metals have $\varepsilon_F \geq 10^4$ K and T_c of a few K, leading to rather small critical fields. For critical fields near 10 Tesla, one requires small Fermi energies, and since $\varepsilon_F = p_F^2/2/m^*$, where m^* is the effective mass, one wants to look at systems with large m^*. This leads one to the study of heavy fermion materials [19]. For example, aluminum has B_{c20} = 0.01 Tesla, while the heavy fermion UBe_{13} has B_{c20} = 10 Tesla.

The B_{c20} value discussed above is due to the occurrence of orbital supercurrents that are formed around the penetrating magnetic-field flux tubes in a *type II* superconductor [18]. Above B_{c20} the superconducting state is lost. Superconductivity can also be destroyed in a magnetic field when the field is strong enough to break the Cooper pairs. This pair-breaking field is known as the paramagnetic critical field $B_p = \Delta/2\mu_B = 1.8\ T_c$ Tesla, in a BCS model [20]. Various novel superconducting states have been predicted in high applied magnetic fields. Maki predicted [21] that the superconducting transition would go from 2nd order to 1st order if $\alpha_M \equiv B_{c20}/(\sqrt{2}\ B_p) \cong 1$, a weak orbital limit. Somewhat before this, a non-uniform superconducting state (FFLO) was predicted [22] to occur in a clean superconductor (electron mean free path >> ξ) with λ >> ξ. The non-uniformity corresponds to the pairing of electrons with a finite net momentum **k**, as contrasted with the |**k**| = 0 in the more typical BCS state. This latter prediction was extended [23] to predict a finite-**k**, non-uniform state for $\alpha_M = 1.16\Delta/\varepsilon_F > 1.8$. The non-uniformity means that the order parameter will depend on spatial

position within the superconductor. Thus, in a transverse field μSR experiment one would expect to see a change of the inhomogeneous linewidth as one raises the field across the phase boundary. One can estimate that the scale of this modulation should be 800 – 1600 Å, well within the measurement range of a μSR experiment.

2.1.2 Magnetism

Magnetism, i.e. the physics of interacting spins in condensed matter, is one of the central topics in solid states physics. The persistent interest in this field is triggered not only by the vast range of technological applications of magnetic systems e.g. in electrical engineering and information storage but also by actual topics in fundamental physics.

In the following Subsections, some examples of research focused on magnetism where a high-field μSR instrument could play an important role are presented.

2.1.2.a Molecular Magnets — High Spin Molecules

Computers save files in a "read/write" format by using magnetic memory. Due to rapid technological advances, the size of this magnetic memory unit decreases every year. Even so, the smallest memory unit to date uses as much as 100 billion atoms to hold one bite of information. This vast number considerably limits the memory capabilities, and a global effort is currently under way to reduce the size of this unit.

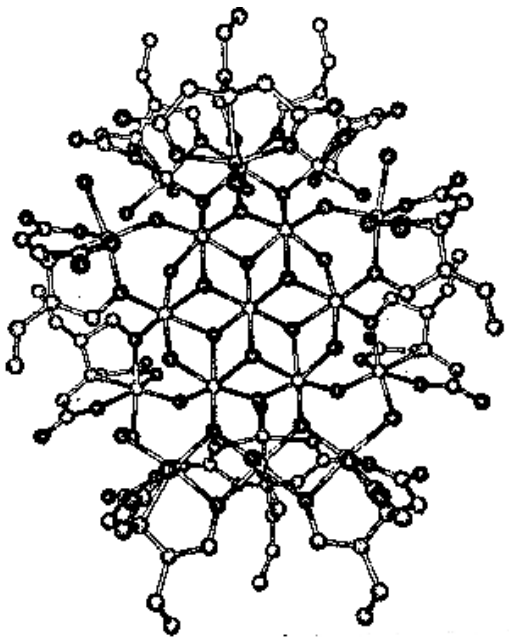

Figure 5 *A disc-like molecular cluster, about a nanometer across, containing 19 iron atoms linked by oxygen atoms with organic molecules tacked around the edge [24].*

One possible solution is to use molecular clusters containing only 10 to 100 atoms. These systems are *high spin molecules*, comprising a small network of magnetic ions in such a way that the net spin of the cluster, *S*, is large (e.g. 10, 27/2 or 39/2). The clusters contain both magnetic ions and organic ligands which bind the magnetic ions into a well-defined geometry. These clusters crystallise in a lattice and the intercluster interactions can largely be ignored. However, there is a major obstacle in this option, which has so far hindered its wide spread use: at this small size such molecules, adhering to the rules of quantum mechanics, could spontaneously reverse the direction of their magnetization and therefore "lose" their memory via quantum tunneling of the magnetization (QTM). Consequently much experimental effort is applied to study the QTM in these molecules.

Various chemically prepared magnetic clusters have recently attracted great interest for studying macroscopic quantum effects [25]. When the temperature is lower than an anisotropy barrier (which lifts the $2S + 1$ degeneracy of the spin S), the only possible spin-relaxation mechanism is quantum mechanical and phenomena such as quantum tunneling of magnetization can be observed.

Experimental studies [26,27,28] show that the muon-spin relaxation is thermally activated at high temperature, but this saturates as the sample is cooled and the resulting temperature-independent muon-spin relaxation at low temperature is indicative of quantum fluctuations. The field dependence of this relaxation allows the quantum tunneling rate to be extracted via the magnetic field dependence of the relaxation. Large magnetic fields would allow this tunneling rate to be extracted more accurately, but will also allow tunneling between levels close to level crossings to be probed (see Figure 6).

This is illustrated by preliminary measurements performed on the high spin molecule $[Fe_8O_2(OH)_{12}(C_6H_{15}N_3)_6]$-$Br_7(H_2O)Br8H_2O$, also known for short as Fe_8. The Fe_8 has a ground state of spin $S = 10$ and the most important terms in the Hamiltonian are given by $H = -DS_z^2 - g\mu_B \boldsymbol{SH}$ where $D = 0.275$K and **H** is the external magnetic field. When the field is applied along the easy axis **z** direction, the energy levels of this Hamiltonian are given by $E(n) = -Dn^2 - g\mu_B nH$, where n is an integer running from –10 to 10. In zero field, the ground state is given by $n = \pm 10$. At certain "matching" magnetic-field values $H_m = 0$; +0.21; +0.42 Tesla etc., states with different n's (e.g. $n = +10$ and $n = -9$) can have identical energies.

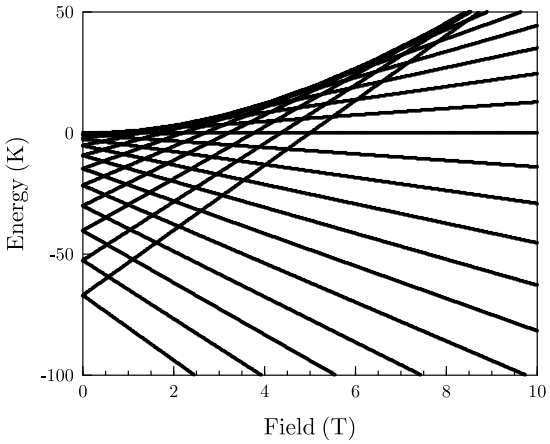

Figure 6 *Energy levels in an S = 10 molecule, Mn_{12}-acetate, as a function of magnetic field. Note the crossing of different energy levels at different fields allowing tunneling between different states.*

Using a multi-step magnetic field cycle (which is indicated in the different panels of Figure 7) it was demonstrated by μSR that specific energy levels can be populated, and that the population can be maintained *over many hours*, eventhough the field was reduced to nearly zero at the end of the cycle. This is demonstrated by small differences of the μSR spectra, although all measurements were performed under the *same final magnetic conditions*. In other words, it was possible to create a multi-bit magnetic memory out of high spin molecules. At this point it could be possible to directly explore the QTM phenomenon between different energy states. However, at present the quality of the data is rather limited by the relatively small magnetic field available at the PSI μSR instruments, with which the different states can be prepared. A significantly higher magnetic field will allow a better differentiation between the different energy levels and field cycles.

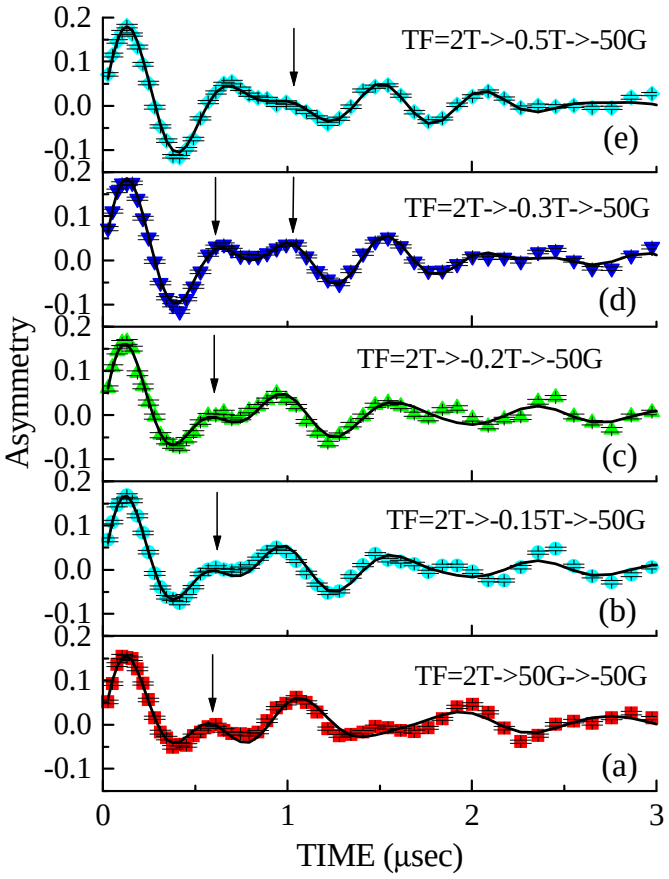

Figure 7 *μSR signal in Fe_8 measured under identical conditions (TF 50 Gauss) but after different magnetic history. Note the differences in the data pointed at by the arrows, indicating that different spin states have been populated.*

2.1.2.b Spin Ladder Systems

Since the advent of high temperature superconductivity the low dimensional quantum magnets, i.e. systems having localized magnetic moments of low effective spin angular momentum (S = 1/2 or S = 1) that interact antiferromagnetically in less than three dimensions, became an intense field of study in magnetism.

Under these specific circumstances quantum fluctuations play an important role and both the ground state properties and fundamental excitations are completely different from the classical picture of long range Curie or Néel order and spin wave propagation. Often non-magnetic spin singlet states with an *excitation gap* of several degrees Kelvin are formed. The spin singlet ground state can be caused by a *structural dimerization* of the spin interaction. This is the case in local "zero dimensional" spin pair compounds or 1-dimensional chain systems with a *spin-Peierls* transition like $CuGeO_3$. On the other hand collective non-magnetic states like the Haldane state in S = 1 chain systems or resonating valence bond liquids in frustrated two-dimensional S = 1/2 lattices can be found [29].

It is mandatory to study the response of these systems in high magnetic fields to identify the actual ground state and to determine the local exchange constants which can be very

strongly renormalized in zero and low magnetic fields due to quantum effects. The main purpose of the high field is to close the excitation gap to the magnetic (triplet) state. In this case quantum phase transitions accompanied by quantum critical behavior of the order parameter and the dynamic correlation functions are expected at low temperatures.

In the following, a few examples of low dimensional quantum magnets will be presented to illustrate the rich physics found in these systems and to outline the potential applications of high field μSR. Since the maximum magnetic field strength anticipated for the future μSR instrument is of the order of 15 Tesla, the actual examples are mostly chosen so that this field range is sufficient to access the critical regime in the magnetic phase diagram.

The term "*n*-leg spin ladders" refers to *n* parallel chains of magnetic ions where the magnetic interchain coupling along the *rungs* is comparable to the couplings along the chains (*legs* of the ladder). In the absence of charge carriers the *even*-leg ladders have a spin gap in the energy spectrum above the singlet ground state. Therefore these systems show an analogous behavior to the underdoped 2-dimensional High-T_c compounds where a pseudo spin gap with a low density of low-energy excitations is observed. Since also superconductivity is observed in a 2-leg ladder material [30] as has been predicted by theory [31], the analogy is even stronger.

For $S = 1/2$ systems the critical field strength B_c in Tesla to close the spin gap is of the order of the excitation gap Δ in Kelvin. For isotropic coupling (i.e. $J_{rung} \approx J_{leg}$) in spin ladders $\Delta \approx 0.5 \cdot J$. Therefore systems which can be studied in high field μSR must have a magnetic coupling J in the 20-30 Kelvin range or below.

An example in this category is the organic two-leg spin ladder $Cu(C_5H_{12}N)_2Br_4$ [see for example 32]. In this system localized $S = 1/2$ spins of the Cu^{2+} ions interact via Br^+ superexchange ($J_{rung} \approx 13$ K, $J_{leg} \approx 4$ K) resulting in an spin gap of $\Delta \approx 9.5$ K. In low temperature magnetization measurements a gapless behavior of a 1-dimensional Heisenberg antiferromagnet is recovered between 6.6 and 14.6 Tesla. A universal scaling of the magnetization indicates quantum critical behavior which can be understood in terms of a Bose condensation of singlets or triplets out of a disordered Luttinger liquid phase.

A similar material discussed as a two-leg $S = 1/2$ spin ladder is $Cu_2(C_5H_{12}N_2)_2Cl_4$ [33] which has been extensively studied recently. Two quantum critical points at $H_{c1} = 7.5$ and $H_{c2} = 13.2$ Tesla have been derived. They correspond to field values where the ground state changes from a *gapped* spin liquid phase to a *magnetic phase* with a gapless ground state and finally to a *fully polarized magnetic gapped phase* [34,35].

The formation of magnetization plateaus is not only possible at zero or full polarization. Several systems show plateaus at fractional magnetization values. Oshikawa et al. [36] have developed a criterion for fractional magnetization plateaus in quantum systems on the base of classical arguments. To check the theoretical predictions more experimental work is necessary. A system accessible with high field μSR is NH_4CuCl_3 [37]. This ladder material exhibits 1-dimensional behavior with a finite susceptibility at low temperature and low magnetic field strength. Between 5 to 12 and 17 to 25 Tesla magnetization plateaus with 1/4 and 3/4 full polarization are found (see Figure 9). The isostructural system $TlCuCl_3$ exhibits a spin gap of 7 K in low field [38]. At a critical field of 6 Tesla an increase of the low temperature magnetization is interpreted as a 3-dimensional condensation of thermally occupied triplets.

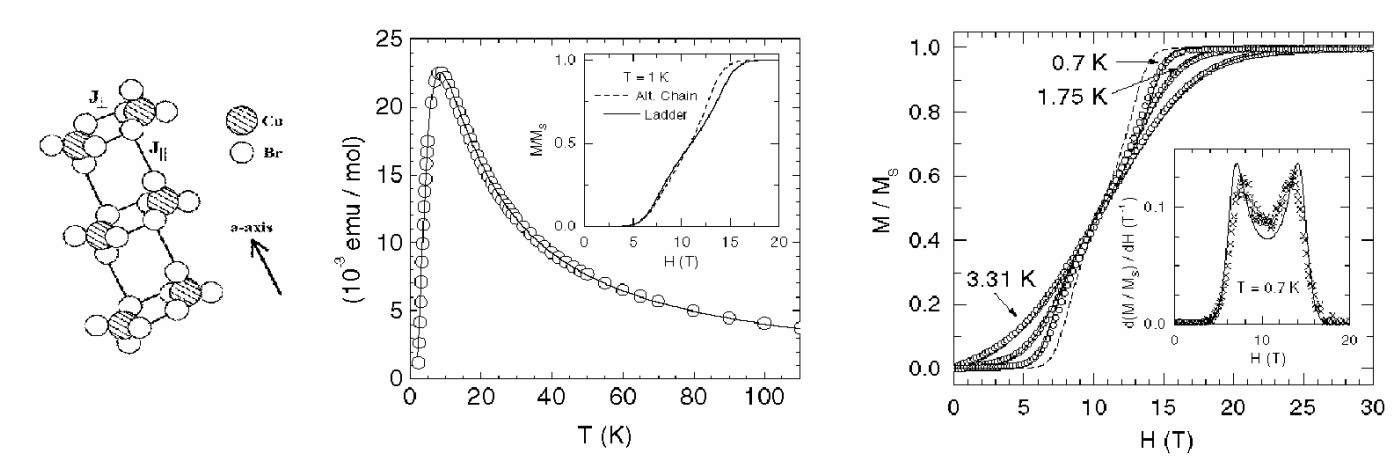

Figure 8 *Cu coordination, magnetic susceptibility and magnetization of $Cu(C_5H_{12}N)_2Br_4$ [32].*

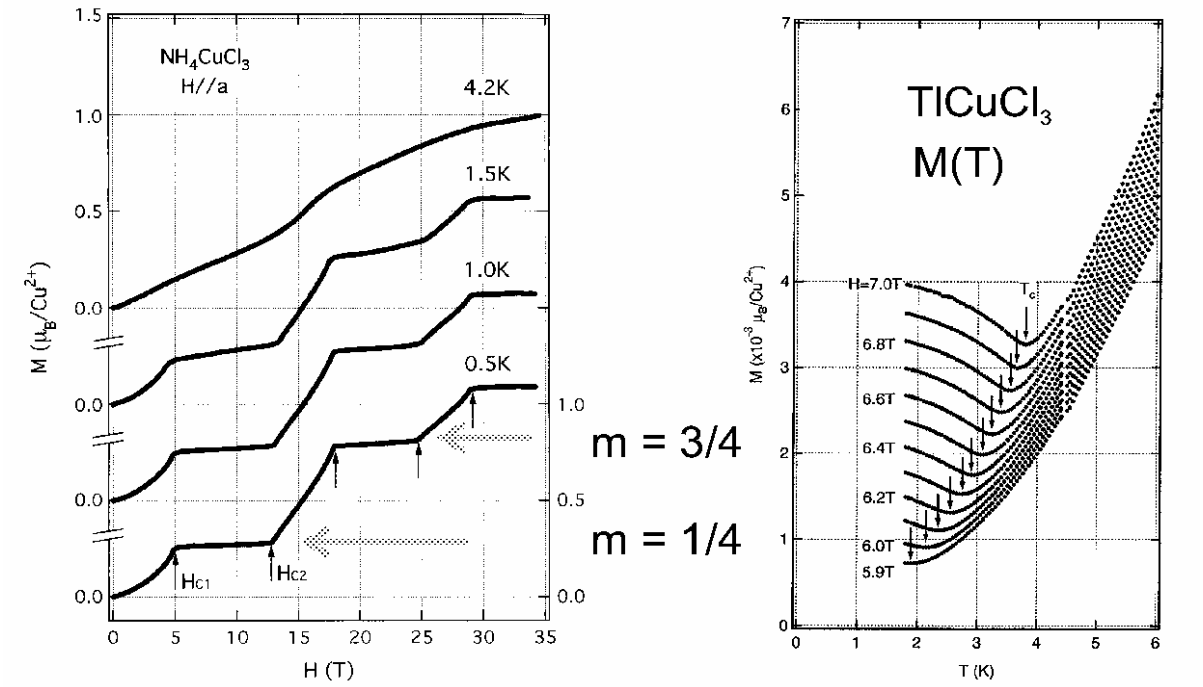

Figure 9 *Low temperature magnetization in NH_4CuCl_3 [37] and $TlCuCl_3$ [38].*

In the examples presented above, there are many open questions which can be addressed with high field μSR. Static properties like the local order parameter and its spatial homogeneity can be derived from muon Knight shift measurements, for which high fields are

required (see Section 2.4.1). On the other hand, the muon spin relaxation, and its field dependence, can be used to measure the correlation function of the spins in the investigated systems. Moreover, the time window accessible by μSR measurements is complementary to other techniques like ESR, NMR and neutron scattering.

2.1.2.c Frustrated 2-Dimensional Systems

In two-dimensional systems the conditions for the formation of nonmagnetic ground states are currently studied very intensively. Quantum phases are observed in the case of competing interactions, i.e. a high degree of frustration and a small coordination number. In this case the magnetic phase diagram can exhibit hysteretic metamagnetic transitions and magnetic plateaus at zero and at rational values of the magnetization as well as complicated magnetically ordered phases like chiral or incommensurate order.

An example for a topologically frustrated system is the triangular lattice with antiferromagnetic interactions. Experimentally this situation is found in Cs_2CuCl_4 which is a spin-1/2 Heisenberg antiferromagnet on a two-dimensional anisotropic triangular lattice with exchange J along b-axis chains and "interchain" zig-zag coupling $J' = J/3$ along the c-direction (see Figure 10) [39]. Neutron scattering experiments reveal a rich magnetic phase diagram very different for magnetic field orientations parallel and perpendicular to the planes [40]. In zero-applied field and due to the frustrated couplings, spins show incommensurate correlations that are stabilized by the finite inter-layer couplings J'' into a true 3-dimensional long-range ordered structure at temperatures below $T_N = 0.62$K: spins rotate in spirals that are nearly contained in the bc-plane by a small anisotropy. Strong quantum fluctuations are directly manifested in large renormalizations (by a factor ca. 2 from classical values) of properties such as the ordering wavevector and the energy scale of the excitations.

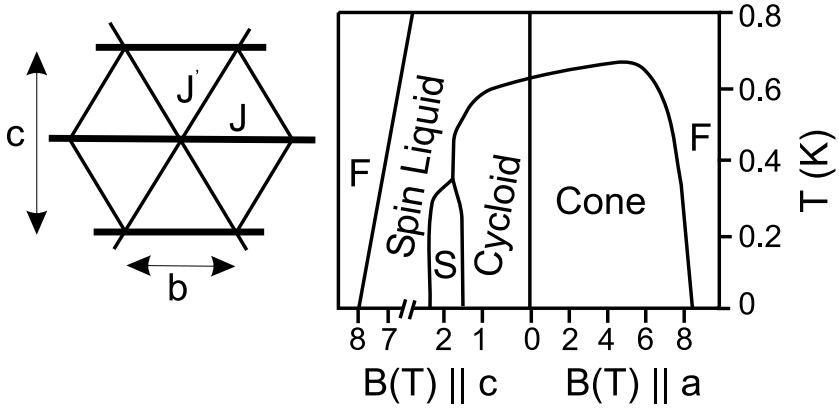

Figure 10 *Triangular magnetic lattice and magnetic phase diagram of Cs_2CuCl_4 (from [40]).*

For magnetic fields perpendicular to the triangular planes a transition to a ferromagnetic ordered phase occurs at 8 Tesla without any quantum disordered intermediate phase. Applying the field in plane along the c-axis leads to a disordered spin liquid phase between 2 and 8 Tesla. Obviously the in-plane magnetic field tends to suppress the 3-dimensional magnetic order and the low dimensional physics is recovered. This is further supported by the observation of a broad spinon-like excitation spectrum in inelastic neutron scattering typical for a dominantly one-dimensional Heisenberg antiferromagnet.

The nature of spin correlations in this essentially zero-temperature quantum ground state is a very important question for current theories of quantum phases in two dimensions and could be probed using μSR if higher fields were available.

2.1.2.d Landau Orbital Magnetism in 2D and 3D Metals

Condon Domains:

While quantum (de Haas – van Alphen) oscillations due to successive filling of Landau levels in metallic systems have long been known and used as standards for mapping Fermi surfaces (FS) [41], a new chapter in this field has been opened by the discovery of the *instability* of the oscillations in certain conditions and the resulting domain structure [42]. For Condon domains, high-field μSR is the only generally applicable tool of investigation. The domains arise periodically, provided the oscillatory magnetic susceptibility $\chi = dM/dB$ has an amplitude $\chi_a > 1/4\pi$. It can be shown that $\chi_a \propto n^k \psi(T/B, T_D/B)$, where the filling number $n = \hbar c A/2\pi eB$ depends on the extremal cross section A of the FS, and the "damping factor" $\psi \leq 1$ is a decreasing function of its arguments (the Dingle temperature T_D characterizes crystal perfection). The exponent is k = 2 or 3/2 for 2-dimensional or 3-dimensional systems respectively, and domains are formed in the field range where $n \approx 10^3$ but where B is large enough (for the given T and T_D) to satisfy $1-\psi << 1$. Previous studies were limited to $H \approx$ 2-3 Tesla, but optimal resolution with μSR is expected in general at higher applied fields, namely at 3 < H < 8 Tesla for Be [43], 8 < H < 30 Tesla for noble metals [44], and 5 < H < 6 Tesla for the quasi-2-dimensional intercalated graphite [45]. There is also a hint for domain formation in the organic conductor β_H-$(ET)_2I_3$ [46] at about 11 Tesla. In spite of recent, promising μSR results (see Figure 11), giving direct evidence for Condon domains in Be and in the polyvalent metals Sn, Al, Pb [43] for fields B < 3 Tesla, the experimental information on the field structure near domain boundaries, the order and kinetics of the diamagnetic transition and the phase diagrams [47,43,44] is still scanty or completely lacking. Considering that this fundamental subject is attracting strong theoretical interest, the need for a spectrometer working in the B > 3 Tesla and T < 1 Kelvin regime would be highly desirable.

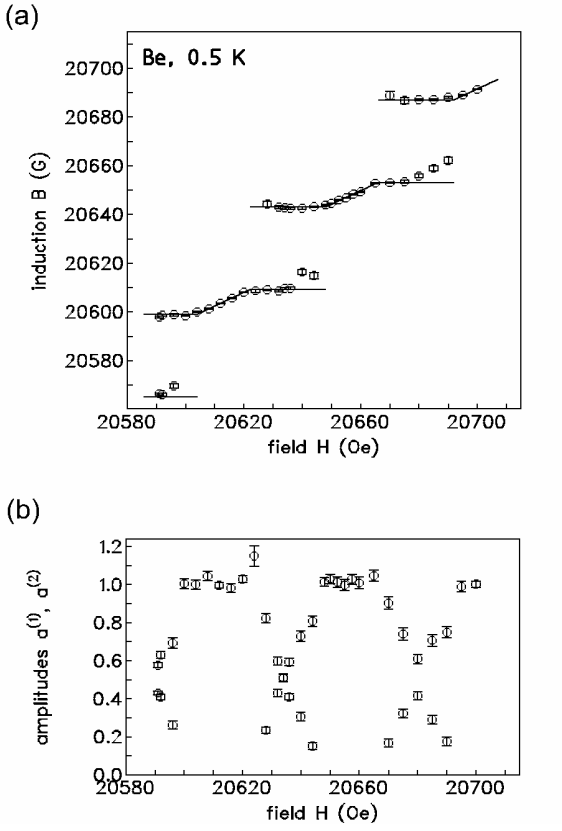

Figure 11 (a) *Domains with opposite magnetizations in Be make the diagram B(H) periodically two-valued;* **(b)** *the line intensities (proportional to the volume fractions of the two kinds of domains) vary linearly with the applied field H [43].*

Internal field in the quantum limit:

In the other limit of low filling numbers (region of the *Integer Quantum Hall Effect*) the cyclotron radius r_c is comparable to the "radius for one electron" $r_e = (3/4\pi\rho)^{1/3}$ and a localization of the orbitals is expected [48] (where ρ is the electron density). This should be observable by μSR, via the increased muon depolarization rate $\sigma \propto B^{1/2}$ due to spatial fluctuation of the internal field [49]. Experiments on Bi [50] indeed showed a systematic increase of σ with *B*, inexplicable through the nuclear dipole fields, and the same was found subsequently [51] in different samples up to *B* = 3 Tesla (see Figure 12). In Bi the quantum limit is attained at *B* = 1.2, 13 or 18 Tesla depending on the field direction, thus possibly on the scale of a future high-field spectrometer.

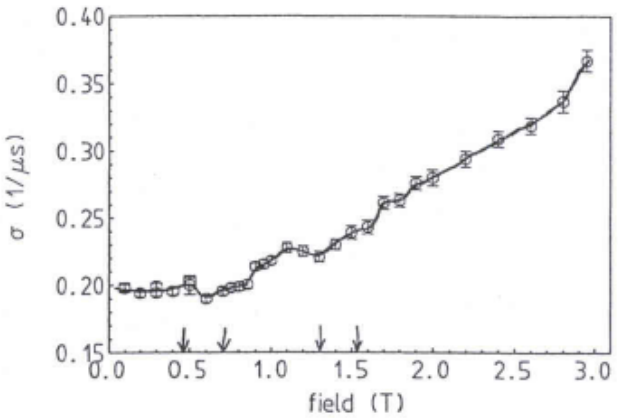

Figure 12 *Measured field dependence of the muon depolarization rate* σ *for Bi, with B||a-axis at 3K. The arrows indicate maxima of the magnetic susceptibility.*

For this research field, the need for high-field μSR here is clear since the *microscopic* study of the quantum limit state, with predominantly localized cyclotron orbitals, is possible in general only by μSR, due to the disturbing skin effect and the quadrupolar interactions e.g. for NMR.

2.1.2.e Heavy-Fermion Systems

In a simple minded model, a heavy-fermion metal can be thought of as a usual metal such as aluminum but with a *strongly renormalized effective mass* for its conduction electrons. This renormalization, which arises from electronic correlations between the conduction electrons and the localized *f*-electrons, can be so large that the effective electron mass m^* is of the order of *200 times* the mass of the free electron, i.e. about the muon mass (for a review see [52]). A fascinating aspect of this class of compounds is the observation that, within the heavy-fermion regime, a wealth of ground states can occur. For example, unconventional superconductivity is observed in a few systems and usually coexists and couples with static magnetism. Also among the heavy-fermion systems, the magnetically ordered states appear rather anomalous and are often characterized by random, incommensurate, or extremely short-range order, sometimes associated with very small static moments. Due to its specific characteristics the μSR technique has been extensively utilized to investigate the peculiar magnetic properties of these systems (for a review see [53]). In the following we report some examples where the use of a high-magnetic field could dramatically improve the specific information extracted from μSR studies on heavy-fermion compounds.

The interplay of magnetism and superconductivity has been a topic of great interest for many decades. This interplay is nicely displayed in several heavy-fermion superconduct-

ing systems, in which magnetic and superconducting order parameters compete, coexist or couple to one another [19]. One such system is $CeCu_2Si_2$, which displays clear evidence of the competition between these two ground states, depending on the stoichiometry and the applied magnetic field [54]. At zero field this system is superconducting below about 0.6K. However in an applied magnetic field the system displays at least two novel magnetic states: the so-called A state, which exists between B = 7 T at zero Kelvin and B = 0 T at 0.6 K, and the B state which is found at fields B > 7 T below about 0.6K. The exact nature of these states is yet to be determined. The µSR Knight shift could be used to probe the local susceptibility of these phases and to more carefully map out the field-temperature phase diagram as a function of stoichiometry, for example. A similar phase diagram has also been found in the heavy fermion superconductor UPd_2Al_3, which is superconducting below about 1.8K and possesses magnetic phases below 12-14K in fields $B \leq$ about 5 T (phase I) and $B \leq$ about 18 T (phase II) [55].

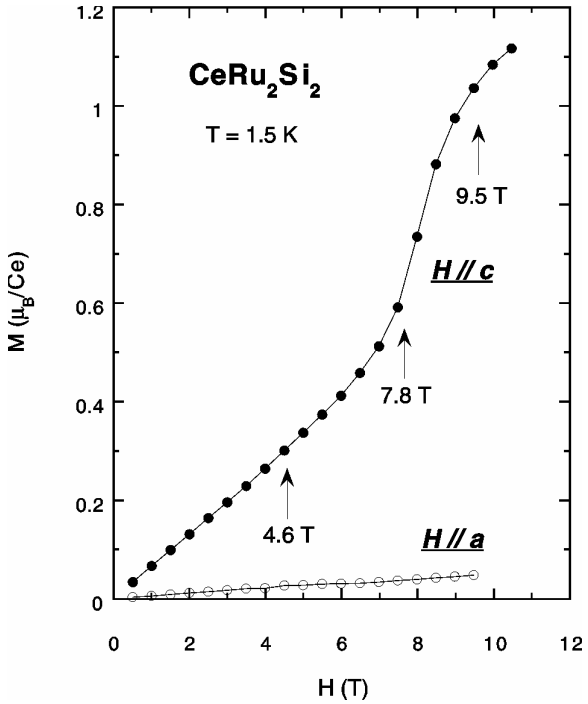

Figure 13 *Magnetization versus the applied field recorded at 1.5 K for $CeRu_2Si_2$; from J.X. Boucherle et al. [56].*

Another model heavy-fermion system is the tetragonal intermetallic $CeRu_2Si_2$, which does not display any signature of a phase transition in bulk measurements. However, a *metamagnetic* transition is observed at low temperature at about 8 T. This transition manifests itself by a clear non-linear magnetization as a function of the applied magnetic field as shown in Figure 13. Interestingly, no change of the elastic neutron cross-section could be observed as a function of field [56]. Therefore it appears that the localized *4f* electron density is not directly at the origin of the metamagnetic behavior. Available µSR data on this system indicate the occurrence of a magnetic signal at very low temperature, which can be attributed to long wavelength itinerant magnetic excitations [57]. Since this µSR signal can also be

observed in transverse field measurements [58], a high magnetic field study should provide more insight in the microscopic origin of the observed metamagnetic transition.

2.1.2.f Colossal Magnetoresistive (CMR) Systems

There is a strong and continuing interest in the CMR manganites [59] which derives from the great variety of competing ground states exhibited by these materials. This unusual variety, which includes ferromagnetic (FM), antiferromagnetic (AFM), insulating, conducting, charge- and orbitally-ordered ground states, arises from the strong interaction between spin, charge and lattice degrees of freedom [60]. The series of $La_{1-x}Ca_xMnO_3$ compounds displays all of the ground states mentioned above in a single crystal structure [61]. When Ca^{2+} is substituted for La^{3+}, Mn^{4+} ions are produced in place of the Mn^{3+} found in $LaMnO_3$. Competing AFM super-exchange and FM double-exchange (between Mn^{3+} and Mn^{4+}) interactions, strong electron-phonon coupling and Coulomb repulsion mediate these transitions [60]. For example, for $0.21 \leq x \leq 0.50$, the system undergoes an insulator-to-metal transition at the ferromagnetic transition temperature T_C. A large change in magnetoresistance also occurs at T_C. Of particular recent interest is that the $x = 0$, 1/2 and 2/3 compounds exhibit both charge and orbital ordering of the Mn 3*d* states. The $Pr_{1-y}Ca_yMnO_3$ materials also exhibit charge ordering [62] which is particularly resistant to applied magnetic fields. $Pr_{0.5}Ca_{0.5}MnO_3$, for example, remains in a charge-ordered state (in which Mn^{3+} and Mn^{4+} ions sit on alternate sites) below about 150 K in fields up to 20 Tesla, depending on whether the field is decreasing or increasing. When $y = 0.4$, however, the charge ordered state is destroyed by fields of the order of 10 Tesla. This would be an ideal system to study the spin dynamics and local magnetic susceptibility using μSR if fields of 10-15 Tesla were available.

2.1.3 Semiconductors / Semimetals

2.1.3.a Korringa Relaxation in Semimetals

The seemingly diamagnetic μSR signals in materials such as Sb and Bi – and even in graphite, which is still used as a reference sample for muon polarization and decay asymmetry – belie complex issues of local electronic structure and dynamics. The electron density in these semimetals is too low to screen the muon charge and suppress muonium formation, as occurs in normal metals. It is spin or charge exchange with the conduction electrons which precludes the observation of long-lived paramagnetic states. Shifts of the Larmor frequency in transverse field are known for these elements. (They are loosely known as Knight shifts [see also Section 2.4.1], but in fact are larger than in simple metals and significantly temperature dependent). Careful measurements reveal that such frequency shifts correlate with longitudinal muon spin relaxation which, although weak, is by no means negligible in these materials [63]. A new theoretical formulation of the Korringa relation (the original was intended to apply only to simple metals at low temperature) promises to provide a framework for interpreting such data, and to relate it to muon depolarization in magnetic metals [64]. The case of graphite further relates it to the case of spin-exchange on organic radicals [65].

Whereas Korringa relaxation for the host nuclei in simple electrons is independent of applied magnetic field, the same is unlikely to be true in semimetals (where the density of

states is minimal and varying strongly at the Fermi energy). None of the preliminary μSR studies have yet been taken above a few hundred mT, so exploration to much higher fields – both of the transverse-field frequency shifts and the longitudinal-field relaxation rates is a high priority. The high-field variation will reveal and characterize the slower electron encounter or exchange rate.

The point here is that screening theory has focused on a static description of the local charge build up. (The theory has also been somewhat neglected of late, perhaps for lack of data.) High-field μSR data in materials with a wide range of conduction electron densities promise to link the static aspects of defect-charge screening to the dynamical aspects of electron exchange and temperature dependence.

The effects of Landau levels and cyclotron orbits in semimetals also require high-field studies. These are dealt with in the Section 2.1.2.d. (See also Section 2.1.3.d below, for a particular case in semiconductors.)

2.1.3.b Electrical Activity of Hydrogen Impurity in Semiconductors

Much of the current understanding of hydrogen impurity in semiconductors comes directly from the use of positive muons to mimic interstitial protons and of muonium to mimic isolated hydrogen defect centres. This is true both of the cystallographic sites involved – notably the unexpected metastability between cage-centre and bond-centre in Si, Ge, GaAs etc. – and of the associated electronic structures. These are all deduced more easily and unambiguously from μSR hyperfine and quadrupole spectroscopy than by any conventional technique and now even extend to the negatively charged centre, mimicking the elusive interstitial hydride ion.

Moving from spectroscopy to dynamical studies, the so-called charge-exchange regime is especially important. It models the electrical activity of hydrogen impurity in terms of rapid capture and loss of electrons [66]. Repeated formation and ionization of muonium provides a powerful relaxation mechanism. It is analysis of the form of the field and temperature dependences which identifies the particular interplay of site and charge state involved. Figure 14 shows TRIUMF data for GaAs [67] where the relaxation rate is still varying strongly at 7 Tesla, maximum field currently available. Higher fields are manifestly required to pursue the studies to faster cycle rates, exploring higher temperatures or higher levels of doping.

The illumination of semiconductors begun at PSI and the muonium response to photogenerated carriers is another major area – so far sadly under-explored – which would likewise benefit from the highest possible applied fields.

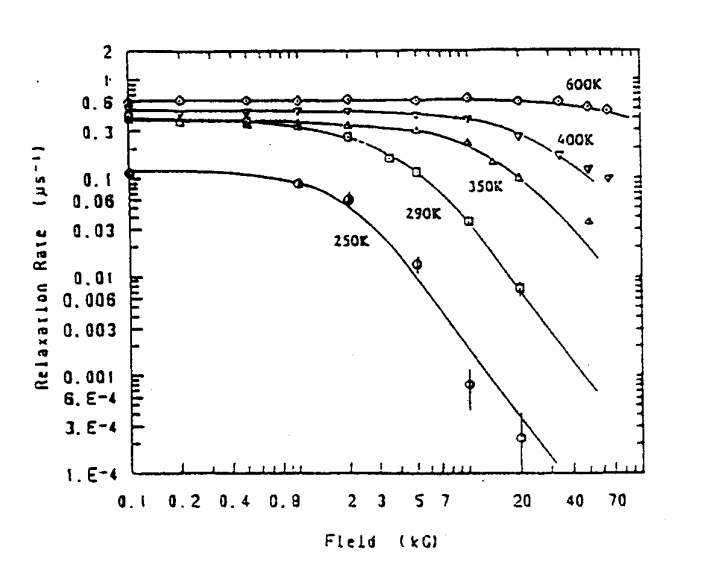

Figure 14 *TRIUMF relaxation rate data for GaAs, still unquenched and varying strongly towards 5 Tesla [67].*

In all such studies, intermittent hyperfine coupling due to muonium spin or charge exchange may be expressed as fluctuations about a static average. The fluctuations cause spin relaxation, both longitudinal (as in Figure 14) and transverse. The static average, which is non-zero in the presence of some electronic spin polarization, in addition produces a paramagnetic shift of the (seemingly diamagnetic) muon Larmor precession signal. One goal here is to demonstrate some generalized Korringa relationship between relaxation rate and frequency shift. Measurements well above room temperature in silicon have revealed serious shortcomings of our present understanding, however. Figure 15 shows PSI data for the frequency shift, which is large enough to be measurable even at temperatures where charge-exchange relaxation is fastest. Nevertheless a consistent set of parameters for electron capture and loss, site change etc., cannot be found to describe both the shift and relaxation data [68].

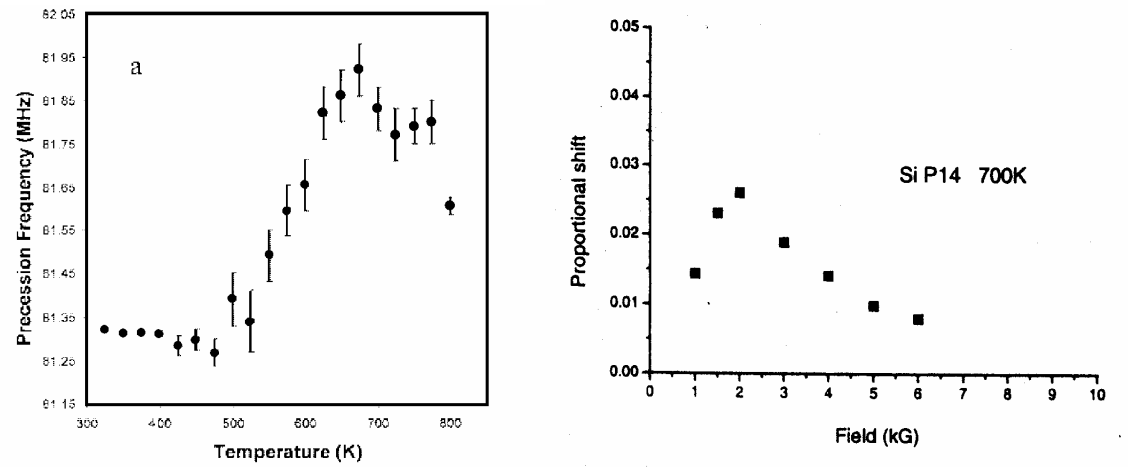

Figure 15 *PSI data showing a huge shift of the muon Larmor frequency in silicon, as a function of temperature [17] and field [18]. The field dependence shows that the assymptotic limit required for reliable analysis has not been reached.*

It has recently become clear from field dependent data [69] that the frequency shift is not a function of electronic polarization alone, *although it must become so at very high fields*. Analytical expressions at low and intermediate fields prove impossible to derive: different mathematical approaches even lead to shifts of opposite sign [70]! The most reliable resolution is to extend the measurements to fields where the mathematical expressions become assymptotically correct, probably between 5 and 10 Tesla, i.e. towards 100 times the hyperfine field for normal muonium in silicon.

The importance of such a study is to see whether the electrical activity of hydrogen impurity at high temperature involves interplay of the same sites and electronic structures as identified by low temperature μSR spectroscopy, or whether new states or processes come into play.

2.1.3.c Shallow Donor Muonium States: Implications for Hydrogen as a Dopant

The characteristic of these low temperature states, for the Group IVelements Si and Ge and for several of the III-V compounds exemplified by GaAs, is that the muonium electron is strongly bound. The corresponding +/0 donor level and –/0 acceptor level both lie deep in the energy gap. As a result, interstitial hydrogen is a compensating defect, trapping electrons in n-type material and releasing them in p-type. That is, it counteracts the conductivity of deliberate dopants. A very exciting new μSR discovery (see Figure 16) is that of very weakly bound states, notably in the II-VI compounds [71, 72]. By implication, hydrogen may then be used as a deliberate dopant to create or control conductivity. This has become a highly topical issue, with first μSR and then ESR/ENDOR data confirming a theoretical prediction for ZnO [73, 74, 75].

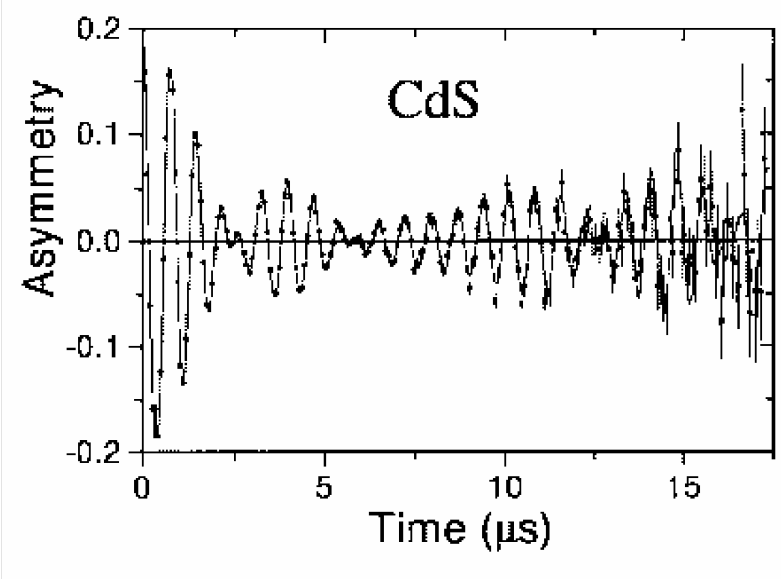

Figure 16 *PSI Muon On REquest (MORE) spectrum for the shallow donor muonium state in CdS [71].*

This new branch of muonium spectroscopy has been facilitated by the weakness of the nuclear magnetism in the II-VI compounds. As similar shallow states are discovered in semiconductors with abundant dipolar nuclei, e.g. InN [76], high transverse fields would be

beneficial in decoupling the adjacent nuclei. High field spectra would clarify measurement of the spin density on the central muon; the decoupling behaviour would characterize the broad distribution of spin density on surrounding nuclei.

2.1.3.d Modelling Astronomically High Fields

The primary characteristics of these shallow donor states are their low binding energy and correspondingly extended hydrogenic wavefunction – the result of low electron effective mass and high dielectric constant. The binding energies are tens of meV in place of the normal hydrogen Rydberg constant of 13.6 eV and in consequence no longer dominate electron Zeeman energies, even in quite modest magnetic fields. The same is shown by the dilated size of the orbits, around 100 times the normal Bohr radius, which is no longer negligible compared with the cyclotron radius. This is another situation in which analytical solutions to the Hamiltonian cannot be found, namely for the precise energy levels when these are intermediate between atomic-like and Landau-like. (Landau levels and cyclotron orbits for *unbound* electrons in semimetals are considered in the Section 2.1.2.d). Far Infrared Spectroscopy on shallow-donor impurities in GaAs, illustrated in Figure 17, have already given unique data [77].

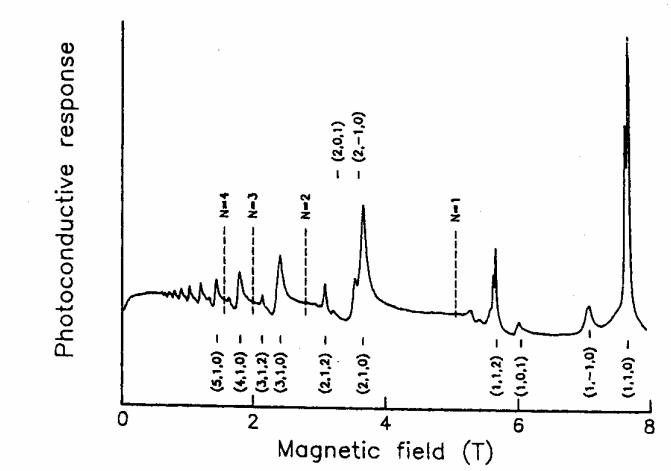

Figure 17 *FIR spectrum of the donor in n-GaAs at 4.2 K [77].*

This inspires the notion that equivalent spectra could be obtained for the new weakly bound muonium states, using trigger detection of laser excitation via the μSR response. Immediate aims here would be to sequence the muonium energy levels and determine their principal quantum numbers. This would distinguish Rydberg from shallow donor states and also permit direct observation of the quadratic Zeeman effect – all highly topical issues [78]. For the donor in GaAs (Figure 17), the magnetic interaction already outweighs the Coulomb interaction in 10 Tesla. For free hydrogen (or muonium) this condition is only reached near 10^6 Tesla [79]. Laboratory data on these shallow donor states would therefore provide a test of the latest mathematical models of these high-field effects, that are otherwise only encountered in the hydrogen-rich interiors of white dwarfs or neutron stars!

2.2 Chemistry

2.2.1 Muonium Adducts to Organometallics

2.2.1.a Motivation

The study of muonium adducts to organic compounds is well developed [80]. Recently, a lot of interest has been devoted to the study of the muonium adducts to organometallics, mainly for the reasons given below.

The dynamics of organic ligands attached to metal centres are of importance for catalysis. For example, metallocene catalysts are now replacing Ziegler-Natta catalysts, making it possible to engineer the properties of polymers by design at a molecular level [81]. The importance of metallocene ring dynamics to polymer engineering has been illustrated by Waymouth and Coates [82]. The rates of metallocene ring reorientation at the temperatures of interest happen to fall within the 10^{-7} to 10^{-11} s time-window, which straddles the accessible timescales of nuclear magnetic resonance (NMR) and quasielastic neutron scattering (QENS). Of the techniques applicable to this time window, Mössbauer spectroscopy is limited to a very few metals and EPR depends on the presence of stable radicals or molecules with unpaired electrons, and some of the latter may be EPR-silent. The lower end of this time window could be accessed using deuterium NMR, which of course needs the synthesis of fully deuterated samples. μSR has the potential to be a *very versatile* technique for this time window, being applicable to all unsaturated systems. It is the open shell radical species that is studied in μSR, not the closed shell parent. However, it appears that there are situations where the extra electron does not change the dynamics of the molecule.

Consider heterogeneous catalysis where metal surfaces are involved. It is not possible to use NMR to study the dynamics of groups such as benzene rings due to the conducting nature of the substrate. Similar problems are encountered in using NMR to study the dynamics of polymer composites containing conducting materials such as graphite. QENS experiments require samples with large surface areas in order to have sufficient material on the surface, and this is not often possible. With the advent of the *slow muon beams*, it is already possible to study thin films, and surfaces may be accessible in the future. Therefore the development of μSR as a method to probe the dynamics of species on metal surfaces is likely to produce uniquely important information on heterogeneous catalysis.

There is also the possibility of making novel organometallic hydride analogues and studying their properties in a rather convenient way. If found to have interesting and useful properties, the hydrides corresponding to these adducts might then be synthesised by suitably designed syntheses. An example of the importance of a hydride adduct to catalysis is the suspected hydride addition which is presently postulated to be responsible for the termination of catalytic activity in the metallocene catalysis of polypropylene formation [83].

2.2.1.b Need of Higher Magnetic Field

Spin-lattice relaxation that is monitored by the muon spin relaxation is in its simplest form due to transitions between the levels 2 and 4 of the Breit-Rabi diagram [84]. The frequency of this energy gap sets the limits for the dynamic processes that are observable by this method. The transition frequency, $\omega_{24} = 2\pi A\sqrt{(1 + x^2)}$, where x is the reduced field in units of hyperfine field and A is the hyperfine frequency (see Figure 18).

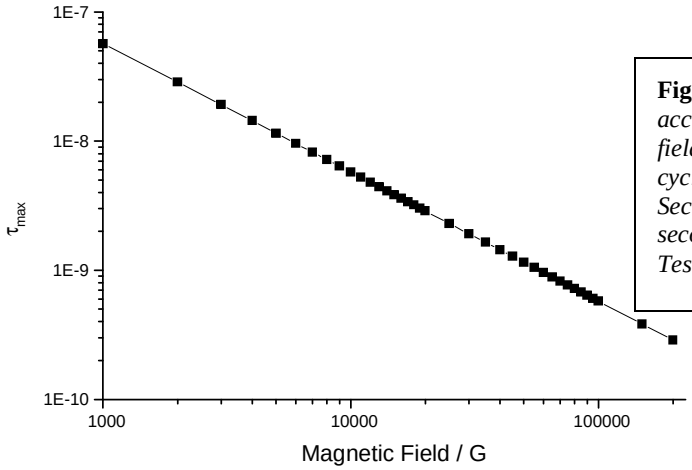

Figure 18 *Plot of the change in the accessible time scales with applied field, assuming a radical similar to the cyclohexadienyl radical (see also Section 2.4.3). The y-axis is given is seconds and the x-axis in Gauss (1 Tesla = 10^4 Gauss).*

Up to now, when studying for example ferrocene, only the low frequency modes, such as the ring rotations, were accessible and provided chemically significant information. Access to shorter time scales will make it possible to use other higher frequency modes that are coupled to the muon relaxation process to be explored. A number of μSR studies are reported for example, on organic molecules of catalytic relevance encapsulated in zeolites [85], liquid crystalline phases [86] and dynamic processes that couple to conduction processes [87]. An extension to the time window of molecular dynamics accessible to μSR should benefit most of these studies.

2.3 Quantum Electrodynamics

2.3.1 Determination of the Negative Muon g-Factor in a Bound State

In Dirac quantum theory the g-factors of the free negative muon and electron are exactly $g_\mu = g_e = 2$. Due to self-interaction with the radiation field, the free muon (electron) possesses an anomalous magnetic moment. Presently, the available measurements of g_μ (g_e) provide an outstanding agreement, at the level of 10^{-10} (10^{-11}), between theory and experiment.

The corrections to the g-factor of the muon (electron) bound in an atom originate not only from interactions with the radiation field, but also from the interactions with the Coulomb field of the nucleus [88, 89, 90, 91]:

$$g_{\mu(e)}^{1s} = 2\,(1 + a_{\mu(e)}^{\text{free}} + a_{\mu(e)}^{\text{QED}} + a_{\mu(e)}^{\text{rel}})$$

where $a_{\mu(e)}^{free}$ is the radiative correction to the *g*-factor of the free muon (electron); $a_{\mu(e)}^{QED}$ is an additional radiative (quantum-electrodynamical) correction for the bound muon (electron); $a_{\mu(e)}^{rel}$ is the relativistic correction for the particle in the 1*s*-state.

Precise measurements of the anomalous *g*-value of a Dirac particle in a bound state provides a sensitive test for the predictions of quantum electrodynamics on the radiative corrections which originate in the Coulomb field. From this point of view the measurements of the *g*-factor of a bound muon may appear to be more preferable than measurements of the *g*-factor of a bound electron. Since the Bohr radius of the muon in the 1*s*-state is 206 times smaller than the Bohr radius of the 1*s*-electron, the Coulomb field on the muon is stronger. As an example, the Coulomb field on the muon in the 1*s*-state of the carbon atom is comparable with the Coulomb field on the 1s-electron in Pb.

According to theoretical calculations [88, 89] the values of a_{μ}^{rel} (a_{μ}^{QED}) for carbon, silicon, zinc and lead are, respectively, $\approx 6\cdot10^{-4}$ ($8\cdot10^{-6}$), $\approx 3.2\cdot10^{-3}$ ($4\cdot10^{-5}$), $\approx 1.1\cdot10^{-2}$ ($1.5\cdot10^{-4}$) and $\approx 3.2\cdot10^{-2}$ ($6\cdot10^{-4}$). But presently, the experimental accuracy (see for example [92]) of the *g*-factor of the bound negative muon appears not sufficient to prove the theoretical predictions made on the a_{μ}^{QED} value. The present experimental accuracy of g_{μ}^{1s} is10^{-4}, 10^{-3} and $\approx 10^{-2}$ for the light (C, O, Mg, Si, S), intermediate (Zn) and heavy atoms, respectively.

The existing experimental data on g_{μ}^{1s} have been obtained by conventional μSR measurements of the muon-spin precession frequency (ω) in a transverse magnetic field (B_{ext}) less than 1 Tesla. As the accuracy of the measurements is proportional to B_{ext}^{-1}, measurements in a magnetic field of 10 Tesla will allow one to determine the magnetic moment of the negative muon in a bound state about *twenty times more precisely* than presently known. This will make it possible to observe experimentally the effect of the quantum-electrodynamical correction a_{μ}^{QED} to the magnetic moment of a bound muon.

2.4 General Comments on the Technique

In this Subsection we very shortly discuss the specific advantages provided by the availability of high magnetic fields regarding the determination of the principal parameters of a μSR experiment.

2.4.1 Knight-shift

When an external magnetic field ($\mathbf{B}_{ext}$) is applied perpendicular to the initial muon-polarization $\mathbf{P}_\mu$ (0), the polarization of a free muon in a metal becomes time-dependent and precesses around the total field $\mathbf{B}_\mu$ at the muon site. By correcting the observed muon-frequency shift

$$K_\mu^* = \frac{\left|\mathbf{B}_\mu\right| - \left|\mathbf{B}_{ext}\right|}{\left|\mathbf{B}_{ext}\right|}$$

for the contribution of the demagnetization and Lorentz field [93] the muon Knight-shift is obtained. This quantity, similar to the NMR Knight-shift, is directly dependent on the local magnetic suceptibility at the muon site and, therefore, the muon can probe the magnetization *distribution* inside a sample (for recent studies see Ref. [94]). The accuracy of the Knight-shift determination is of course directly dependent on the available magnetic field value, and values of the order of 15 Tesla will particularly be helpful by allowing a systematic determination of the muon localization in crystallographic lattice. This determination is mandatory to extract quantitative information from the μSR data.

2.4.2 Fluctuations and Correlations

The manner in which field scans of the muon relaxation rate display the power spectrum of the responsible fluctuations is well known: it follows phenomenology developed in the early days of magnetic resonance [95, 96]. In the case where magnetic or motional perturbations have a Lorentzian spectral density function and induce a simple spin-flip of the muon probe, the field dependence of the relaxation rate is a one-to-one map of this function. The faster the magnetic fluctuations or motional hop rate, the higher the field required to suppress the relaxation and to define the relevant correlation time, as shown in Figure 19.

As a rule, fields up to 15 Tesla would extend the window on correlation time down to $\tau = 1/\omega_\mu \approx 1 \cdot 10^{-12}$ s.

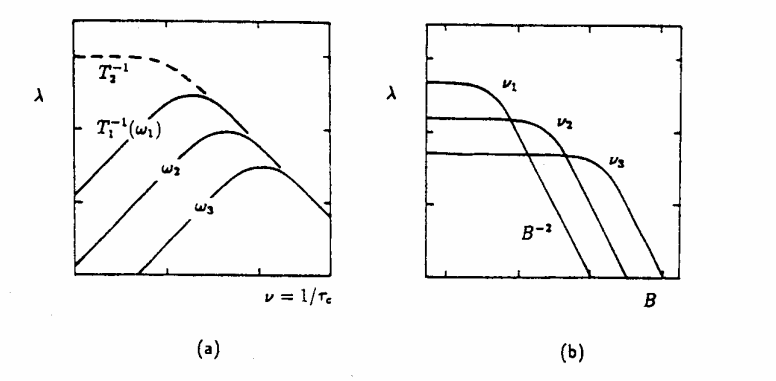

Figure 19 *Variation of the BPP [95] relaxation rate with (a) fluctuation rate and (b) magnetic field. The scales are logarithmic, marked in decades. The peaks in (a) and shoulders in (b) correspond to the condition* $\omega_\mu \tau = 1$.

2.4.3 Molecular Dynamics

When the probe is atomic muonium, or one of its derivative defect centres or molecular radicals, the greater magnetic moment of the electron spin which comes into play generally means that fields up to 15 Tesla will explore correlation times down to $\tau \approx 1/\omega_e \approx$ 0.1 ps. However, the field dependence invariably becomes more complex, since the number of transitions contributing to the observed relaxation now proliferates. Different selection rules apply to different relaxation mechanisms, e.g. diffusion, inter or intra molecular motion, hindered rotation or reorientation, spin or charge exchange. The contribution of each transition is weighted by a squared matrix element which is specific to the perturbation in question and often itself field-dependent, as well as by the appropriate spectral density function [98, 99]. As a consequence, field scans up to at least 10-15 Tesla would be enormously helpful to identify or distinguish dynamical processes as illustrated in Figure 20.

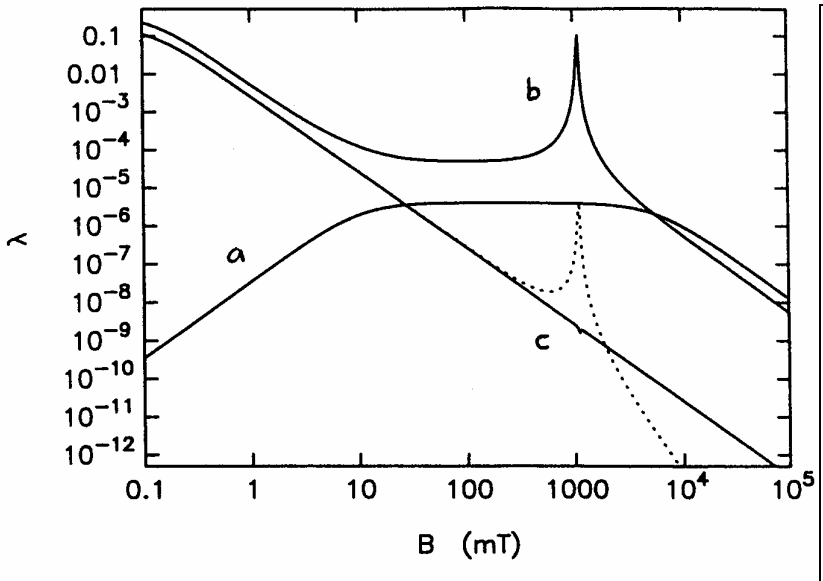

Figure 20 *Field dependences of the longitudinal relaxation rate for muonium or muoniated radicals [97], distinguishing fluctuation of (a) the contact interaction, (b) anisotropic components of the muon-electron hyperfine interaction and (c) a local field. Respectively, these mechanisms apply to (a) intramolecular dynamics, (b) radical reorientation or hindered rotation and (c) muonium diffusion and radical intermolecular motion. This latter case gives the solid line when the effective field interacts equally with the electron and muon, as for the spin-rotation interaction in radicals, or the dotted line when it interacts only with the electron, as for nuclear superhyperfine couplings.*

References

[1] See: PSI Annual Report 1999
[2] **http://μSR.triumf.ca/**
[3] See e.g. Ichioka *et al.*, Phys Rev B59, 8902, (1999).
[4] Kealey *et al.*, Phys. Rev. Lett. 84, 6094, (2000).
[5] J.E. Sonier *et al.*, Rev. Mod. Phys. 72, 769 (2000).
[6] J.E. Sonier *et al.*, Phys. Rev. Lett. 83, 4156 (1999).
[7] J.E. Sonier *et al.*, Phys. Rev. Lett. 79, 1742 (1997).
[8] A. Yaouanc *et al.*, to be published.
[9] J. Singleton, Rep. Prog. Phys. 63, 1111 (2000).
[10] S. L. Lee *et al.*, Phys. Rev. Lett. 79, 1563 (1997).
[11] F. L. Pratt *et al.*, Synth. Met. 120, 1015 (2001).
[12] J. Singleton *et al.*, Phys. Rev. Lett. 88, 037001 (2002).
[13] G. Solt *et al.*, Phys. Rev. Lett. 76, 2575 (1996).
[14] S. Uji *et al.*, Nature 410, 908 (2001).
[15] L. B. Balicas *et al.*, Phys. Rev. Lett. 8706, 7002 (2001).
[16] O. Cépas *et al.*, Phys. Rev. B 65, 100502(R) (2002).
[17] S. Uji, C. Terakura *et al.*, Phys. Rev. B 65, 113101 (2002).
[18] M. Tinkham, *Introduction to Superconductivity*, (McGraw-Hill, Inc., 1996).
[19] R. H. Heffner and M. R. Norman, Comments in Condensed Matter Physics 17, 361 (1996).
[20] A. M. Clogston, Phys. Rev. Lett. 9, 266 (1962).
[21] Kazumi Maki, Phys. Rev. 148, 362 (1966).
[22] P. Fulde and R. Farrel, Phys. Rev. 135, A550 (1964); A. I. Larkin and Y. N. Ovchinnidov, Sov. Phys. JETP 20, 762 (1965).
[23] L.W. Gruenberg and L. Gunther, Phys. Rev. Lett. 16, 996 (1966).
[24] J. C. Goodwin *et al.*, J. Chem. Soc. Dalton Trans. 1835 (2000).
[25] W. Wernsdorfer, Adv. Chem. Phys. 118, 99 (2001); W. Wernsdorfer and R. Sessoli, Science 284, 133 (1999); W. Wernsdorfer *et al.*, Nature 416, 406 (2002).
[26] Z. Salman *et al.*, Physica B 289, 106 (2000).
[27] S. J. Blundell *et al.*, *Proceedings of ISCOM 2001, Hokkaido,* to be published in Synth. Met.
[28] Z. Salman *et al.*, Phys. Rev. B 65, 132403 (2002).
[29] C. Lhuillier, G. Misguich, cond-mat/0109146 (2001).
[30] M. Uehara *et al.*, J. Phys. Soc. Jap. 65, 2764 (1996).
[31] M. Sigrist et al., Phys. Rev. B49, 12058 (1994).
[32] B.C. Watson *et al.*, Phys. Rev. Lett. 86, 5168 (2001).
[33] S. Katano *et al.*, Phys. Rev. Lett. 82, 636 (1999).
[34] G. Chaboussant *et al.*, Phys. Rev. Lett. 80, 2713 (1998).
[35] G. Chaboussant *et al.*, Phys. Rev. Lett. 79, 925 (1997).
[36] M. Oshikawa *et al.*, Phys. Rev. Lett. 78, 1984 (1997).
[37] K. Takatsu *et al.*, J. Phys. Soc. Jap. 66, 1611 (1997)
[38] A. Oosawa *et al.*, Phys. Rev. B 63, 134416 (2001).
[39] R. Coldea *et al.*, Phys. Rev. Lett. 88, 137203 (2002).
[40] R. Coldea *et al.*, Phys. Rev. Lett. 86, 1335 (2001).
[41] D. Shoenberg, *Magnetic oscillations in metals* (Cambridge University Press, Cambridge) 1984.
[42] J.H. Condon, Phys. Rev. 145, 526 (1966).
[43] G.Solt *et al.*, Phys. Rev. B59, 6834 (1999) and Phys. Rev. B 62, R11933 (2000).
[44] A. Gordon *et al.*, Solid State Comm. 103, 167 (1997).
[45] R.S. Markiewicz *et al.*, Phys. Rev. Lett. 54, 1436 (1985).
[46] J. Wosnitza, *Fermi surfaces of low-dimensional organic metals and superconductors* (Springer, Berlin) 1996.

[47] M.A. Itskovsky *et al.*, Phys. Rev. B55, 5636 (1997).
[48] R.E. Prange *et al., The Quantum Hall Effect* (Springer, Berlin) 1987.
[49] G. Solt, Physics Lett. A189, 390 (1994).
[50] E. Lippelt *et al.*, Phys.Rev.Lett. 67, 2525 (1991), and E. Lippelt, ETHZ-Thesis 1990
[51] G. Solt *et al.*, Hyperfine Inter. 104, 369 (1997).
[52] N. Grewe and F. Steglich, in *Handbook on the Physics and Chemistry of rare Earths*, edited by K.A. Gschneider Jr. and L. Eyring (North Holland, Amsterdam, 1991), Vol. 14, P.343.
[53] A. Amato, Rev. Mod. Phys. 69,1119 (1997).
[54] G. Bruls *et al.*, Phys. Rev. Lett. 72, 1754 (1994).
[55] B. Wolf *et al*., Physica B211, 233 (1995).
[56] J.X. Boucherle *et al.*, J. Phys. Condens. Mat. 13, 100901 (2001).
[57] P. Dalmas de Réotier and A. Yaouanc, unpublished.
[58] A. Yaouanc *et al*., Physica B 259-261, 126 (1999).
[59] See for example: *The Physics of Manganites*, eds. T. A. Kaplan and S. D. Mahanti (Kluwer Academic/Plenum, New York, 1999);
Colossal Magnetoresistive Oxides, Advances in Condensed Matter Science, Vol 2, ed. Yoshimori Tokura (Gordon and Breach, The Netherlands, 2000).
[60] A. J. Millis *et al*., Phys. Rev. Lett. 74 (1995) 5144; Phys. Rev. B54 (1996) 5389; Phys. Rev. B 54, 5404 (1996);
H. Röder *et al*., Phys. Rev. Lett. 76, 1356 (1996).
[61] Sang-Wook Cheong and Harold Y. Hwang, in *Colossal Magnetoresistive Oxides* (Ref. 59) p. 237.
[62] M. Tokunaga *et al*., Phys. Rev. 57, 5259 (1998).
[63] S.F.J. Cox *et al.*, Physica B 289-290, 594 (2000).
[64] S.J. Blundell and S.F.J. Cox, J. Phys. Cond. Matter 13, 2163 (2001).
[65] S.F.J. Cox *et al.*, J. Phys. Cond. Matter 13, 2169 (2001).
[66] K.H. Chow, Thesis, University of British Columbia (1994).
[67] R.L. Lichti *et al.* (TRIUMF data, unpublished).
[68] S.F.J. Cox *et al.*, J. Phys. Cond. Matter 13, 2155 (2001).
[69] PSI μSR Experiment RA-98-17 (Report, November 2001).
[70] M. Senba, unpublished.
[71] J.M. Gil *et al.*, Phys. Rev. Lett. 83, 5294 (1999).
[72] J.M. Gil *et al.*, Phys. Rev. B 64, 075205 (2001).
[73] S.F.J. Cox *et al.*, Phys. Rev. Lett. 86, 2601 (2001).
[74] D.M. Hofmann *et al.*, Phys. Rev. Lett. 88, 045504 (2002).
[75] C.G. Van de Walle, Phys. Rev. Lett. 85, 1012 (2000).
[76] E.A. Davis *et al.* (ISIS data, 2001, unpublished).
[77] T.O. Klassenn *et al.*, C. R. Acad. Sci. Paris 323, 187 (1996).
[78] V.G. Storchak *et al.*, Phys. Lett. A 290, 181 (2001).
[79] See for instance: P.W. Barmby *et al.*, Phys. Rev. B 57, 9682 (1998).
[80] D.C. Walker, *Muon and Muonium Chemistry* (Cambridge University Press, Cambridge, 1983);
E. Roduner, *Lecture Notes in Chemistry*, Vol. 49 (Springer, Heidelberg 1988);
For journal special issues on this topic see; Appl. Magn. Reson., 13 (1997) and Magn. Reson. Chem., 38 (2000).
[81] K. Richardson, Chemistry in Britain 1994, 87;
A.D. Horton, Trends in Polymer Science, 2, 158 (1994);
A.M. Thayer, Chemical & Engineering News, 73, 20 (1995).
[82] R.M. Waymouth and G.W. Coates, Science 267, 222 (1995).
[83] See for example: H-H. Brintzinger *et al.*, Angew. Chem. Int. Ed. Engl. 34, 1143 (1995).
[84] See for example: E. Roduner, in *Muon Science: Muons in Physics, Chemistry and Materials*, eds. S.L Lee, S.H. Kilcoyne, R. Cywinski, (Institute of Physics Publishing, Bristol, 1999) p. 173.
[85] E. Roduner *et al*., J. Phys. Chem. A 102, 7591 (1998);
C.J. Rhodes *et al.*, Magn. Reson. Chem. 38, 729 (2000).
[86] B.W. Lowett *et al.*, Phys. Rev. B 63, 54204 (2001).

[87] F.L. Pratt *et al.*, Phys. Rev. Lett., 79 (1997) 2855.
[88] K.W.Ford, J.G.Wills, Nucl.Phys. 35, 295 (1962).
[89] K.W.Ford *et al.*, Phys.Rev. 129, 194 (1963).
[90] S.G.Karshenboim *et al.*, JETP 9, 477 (2001).
[91] A.P.Martynenko, R.N.Faustov, JETP 93, 471 (2001).
[92] T.N.Mamedov *et al.*, JETP 93, 941 (2001).
[93] A. Schenck, *Muon Spin Spectroscopy: Principles and Applications in Solid State Physics* (Adam Hilger, Bristol, UK, 1985).
[94] A. Schenck *et al.*, Phys. Rev. Lett. 89,37201 (2002).
[95] N. Bloembergen, E.M. Purcell and R.V. Pound, Phys Rev 73, 679 (1948).
[96] A. Abragam, *Principles of Nuclear Magnetism* (Oxford University Press, Oxford, 1961).
[97] D.S. Sivia, (2002, unpublished).
[98] S.F.J. Cox *et al.*, Appl Magn Reson 12, 213 (1997) 213; see also Hyp Int 87, 971 (1994).
[99] S.F.J. Cox, in *Muon Science: Muons in Physics, Chemistry and Materials*, eds. S.L Lee, S.H. Kilcoyne, R. Cywinski, (Institute of Physics Publishing, Bristol, 1999) p. 239.